International Journal of Power Electronics and Drive Systems (IJPEDS)
Vol. 12, No. 3, September 2021, pp. 1472~1481
ISSN: 2088-8694, DOI: 10.11591/ijpeds.v12.i3.pp1472-1481

Hybrid nonlinear control strategies for performance enhancement of a doubly-fed induction aero-generator: design and DSP implementation

Bouchaib Rached, Mustapha Elharoussi, Elhassane Abdelmounim
Hassan First University of Settat, FST, Mathematics, Computer and Engineering Sciences Laboratory (MISI), Team: Signal Analysis and Information Processing (ASTI), Morocco

Article Info

Article history:

Received Aug 30, 2020
Revised Jun 18, 2021
Accepted Jul 8, 2021

Keywords:

Backstepping control
Doubly fed induction generator
DSP
HIL
Sliding mode control

ABSTRACT

This paper reports on the design and implementation in DSP as hardware in the loop of a nonlinear control strategy for a grid-connected variable speed wind turbine using a doubly fed induction generator (DFIG). The objective of this work is to build a real-time nonlinear hybrid approach combining Backstepping control and sliding mode control strategies for DFIG used in wind energy conversion systems (WECS). The results of the DSP implementation are discussed and qualitative and quantitative performance evaluations are performed under various disturbed conditions. The implementation is performed using the TMS320F28335 DSP combined with the MATLAB/Simulink (2016a) environment. The experimental results have been satisfactorily achieved, which implies that the proposed strategy is an efficient and robust approach to monitor the WECS.

Corresponding Author:

Bouchaib Rached
Physics and Engineering Science Department
Hassan 1st University, Morocco
Email: bouchaib.rached@gmail.com

NOMENCLATURE

V_{wind}	:	Wind speed
ρ	:	Air density
R_{pale}	:	Blade radius
R_s (R_r)	:	Stator rotor resistance
L_s (L_r)	:	Stator rotor self-inductance
M	:	Mutual inductance
ω_r , ω_s	:	Slip and stator angular velocity
V_{sd} , V_{sq}	:	Stator voltage
V_{rd} , V_{rq}	:	Rotor voltage
I_{sd} , I_{sq}	:	Direct and quadrature stator current
I_{rd} , I_{rq}	:	Direct and quadrature rotor current
I_{gd} , I_{gq}	:	Direct and quadrature filter current
ϕ_{id} , ϕ_{iq}	:	Flux linkage (i=s,r)

1. INTRODUCTION

Continued rising energy demand, declining fossil fuel sources and preoccupation about environmental pollution levels are the main motivations for generating electricity from renewable energy sources. Renewable energies such as solar and wind power are clean, inexhaustible and environmentally

friendly. For these reasons, wind power generation has attracted a great deal of interest in recent years [1], [2].

Several types of electrical machines have been used for energy conversion. However, it would seem that the asynchronous machine is the obvious option in applications using wind turbines. Fixed speed asynchronous machines have to operate around the synchronous speed, because the frequency is imposed by the grid, and the rotor speed is practically constant. The interest of variable speed for a wind energy system is to be able to operate over a wide range of wind speed and to be allowed to get the maximum power from it through the MPPT (maximum power point tracking) strategy, for each speed, for this type of application DFIG associated with power electronics converters is today the most employed machine [3].

These electrical machines have external disturbances, nonlinearities and parametric errors. Conventional linear methods are becoming ineffective, unable to accommodate such phenomena and often give less satisfactory results [4]-[6]. To overcome this problem, the trend in current research has been towards robust nonlinear system controls that give acceptable performances over wide operating ranges. There are many methods developed in the literature use the Robust control to command these systems. The following can be cited as examples the H-infinite control methods [7], [8], the predictive control [9], the fuzzy logic control methods [10]-[16], non-linear control by static or dynamic state feedback [11]-[13], the variable structure control methods [14], [15]. However, the majority of these methods require a lot of calculations and are not really adapted to the WECS-based DFIG control. Only the variable structure control, more commonly called sliding mode control, and the backstepping control seem to be suitable for this topic [14]-[25].

In recently published studies [14]-[25], it has been shown that backstepping control and sliding mode control have given interesting results in terms of robustness and the quality of the produced power. In the present work, the authors intend to improve the performance of DFIG in wind power generation by designing a real-time non-linear hybrid approach combining backstepping control (BC) and sliding mode control (SMC) strategies mainly for robustness to WECS parameter variations, taking into account the non-linearity of the system model. Hardware-in-the-loop (HIL) simulation is a technology that has been emerging in recent years. It consists of validating the developed control laws without the need to use the physical system, it is enough to have a simulated model of the system in question. HIL simulation is therefore widely used in the design of controllers. HIL testing is proving to be an important and universally accepted tool for the control and design of system equipment and power electronics [14]-[27].

The paper is structured in the following way: the Section 2 is devoted to the Methods and Materials. This section is divided to 3 parts. In part 1, the WECS configuration will be presented by establishing the models of the different elements constituting the WECS. The control strategies are carefully elaborated in part 2. The DSP implementation in the loop is presented in part 3. Section 3 is devoted to the results of the validation of the implemented controls.

2. METHODS AND MATERIALS

2.1. Modelling of the wind turbine conversion chain based on a DFIG

A description of the different components of the DFIG-based WECS is shown in Figure 1. The structure of the system can be divided into two main parts. The mechanical part which consists of the turbine, the gearbox and the drive shaft. Then, the electrical part which is composed of the DFIG whose stator is connected directly to the electrical grid, as long as the rotor is connected to the grid by two static bidirectional power converters and a DC bus in a configuration called Back to Back.

2.1.1. Wind turbine

The aerodynamic torque, which is converted by a wind turbine, depends on the power coefficient Cp. It is given by:

$$T_{aero} = \frac{P_{aero}}{\Omega_t} = \frac{1}{2} \cdot C_P(\lambda, \beta) \cdot \rho \cdot S \cdot \frac{V_{wind}^3}{\Omega_t} \quad (1)$$

The ratio λ is expressed by the (2) relation:

$$\lambda = \frac{\Omega_t \cdot R_{Pale}}{V_{Vent}} \quad (2)$$

By applying the fundamental of dynamics, we get the evolution of mechanical speed (the rigidity is very low it can be neglected) [14]-[20]:

$$J \cdot \dot{\Omega}_m = T_m - K \cdot \Omega_m - T_{em} \tag{3}$$

2.1.2. DFIG model

The electrical equations of the DFIG in the Park frame are written as [17]-[21]:

$$\begin{cases} V_{sd} = R_s I_{sd} + \frac{d}{dt}\Phi_{sd} - \omega_s \Phi_{sq} \\ V_{sq} = R_s I_{sq} + \frac{d}{dt}\Phi_{sq} + \omega_s \Phi_{sd} \\ V_{rd} = R_r I_{rd} + \frac{d}{dt}\Phi_{rd} - \omega_r \Phi_{rq} \\ V_{rq} = R_r I_{rq} + \frac{d}{dt}\Phi_{rq} + \omega_r \Phi_{rd} \end{cases} \text{ and } \begin{cases} \Phi_{sd} = L_s I_{sd} + M I_{rd} \\ \Phi_{sq} = L_s I_{sq} + M I_{rq} \\ \Phi_{rd} = L_r I_{rd} + M I_{sd} \\ \Phi_{rq} = L_r I_{rq} + M I_{sq} \end{cases} \tag{4}$$

$$\begin{cases} P_s = v_{sd} \cdot I_{sd} + v_{sq} \cdot I_{sq} \\ Q_s = v_{sq} \cdot I_{sd} - v_{sd} \cdot I_{sq} \end{cases} \text{ and } \begin{cases} P_r = v_{rd} \cdot I_{rd} + v_{rq} \cdot I_{rq} \\ Q_r = v_{rq} \cdot I_{rd} - v_{rd} \cdot I_{rq} \end{cases} \tag{5}$$

$$T_{em} = pM\left(I_{rd} I_{sq} - I_{rq} I_{sd}\right) \tag{6}$$

To be able to easily control the wind turbine's output, the coordinate system (d-q) is oriented to align the d-axis with the stator flux ϕs:

$$\begin{cases} P_S = -V_S \frac{M}{L_S} I_{rq} \\ Q_S = \frac{V_S \Phi_S}{L_S} - \frac{V_S M}{L_S} I_{rd} \end{cases} \tag{7}$$

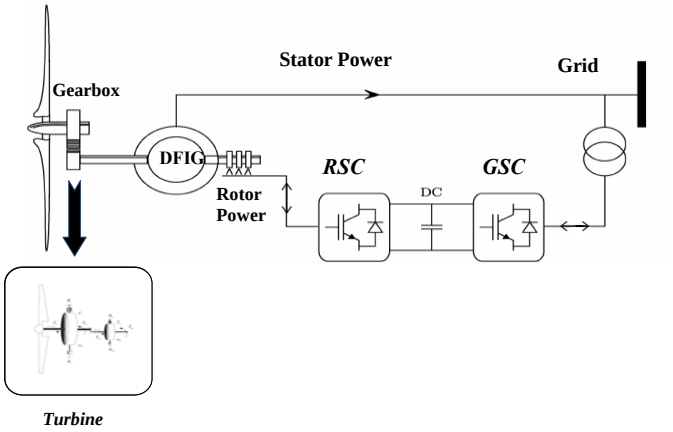

Figure 1. The DFIG-based wind conversion chain

2.2. A hybrid backstepping-sliding mode control of the DFIG powers used in WECS

In this part, we focus on the application of the backstepping method associated with the sliding mode control of the double-feed induction generator. We" ll establish the command value expressions based on the established model in the previous section.

2.2.1. Rotor-side converter (RSC)

The backstepping's command law expressions are as [25]:

$$\begin{cases} V_{rq}^{ref} = \sigma L_r \left[k_2 e_2 + \frac{dI_{rq}^{ref}}{dt} + \frac{1}{\sigma L_r}\left(R_r I_{rq} + \sigma L_r \omega_r I_{rd} + \frac{gMV_s}{L_s}\right) \right] \\ V_{rd}^{ref} = \sigma L_r \left[k_1 e_1 + \frac{dI_{rd}^{ref}}{dt} + \frac{1}{\sigma L_r}\left(R_r I_{rd} - \sigma L_r \omega_r I_{rq}\right) \right] \end{cases} \tag{8}$$

With

$$\begin{cases} I_{rq}^{ref} = -P_s^{ref} \cdot \frac{L_s}{\omega_s M \Phi_{sd}} \\ I_{rd}^{ref} = -Q_s^{ref} \cdot \frac{L_s}{MV_s} + \frac{\Phi_{sd}}{M} \end{cases} \text{and} \begin{cases} e_1 = I_{rd}^{ref} - I_{rd} \\ e_2 = I_{rq}^{ref} - I_{rq} \end{cases} \quad (9)$$

The expression of the backstepping stabilizing command associated with the sliding mode setting is derived as:

$$\begin{cases} V_{rq}^{ref} = \sigma L_r \left[\frac{dI_{rq}^{ref}}{dt} + \frac{1}{\sigma L_r} (R_r I_{rq} + \sigma L_r \omega_r I_{rd} + \frac{gMV_s}{L_s}) \right] + \sigma L_r (k_5 e_1 + k_{71} sign(e_1)) \\ V_{rd}^{ref} = \sigma L_r \left[\frac{dI_{rd}^{ref}}{dt} + \frac{1}{\sigma L_r} (R_r I_{rd} - \sigma L_r \omega_r I_{rq}) \right] + \sigma L_r (k_6 e_2 + k_{61} sign(e_2)) \end{cases} \quad (10)$$

Where k_5, k_{51}, k_6, and k_{61} are positives constants.
To ensure the convergence of Lyapunov's candidate function, we must have verified that:

$$-k_5 e_5^2 - k_{51} e_5 sign(e_5) - k_6 e_6^2 - k_{61} e_6 sign(e_6) < 0 \quad (11)$$

2.2.2. Grid-side converter (GSC)

The backstepping's command law expressions are as [25]:

$$\begin{cases} V_{gd}^{ref} = -L \left[k_3 e_3 + \frac{dI_{gd}^{ref}}{dt} + \frac{R}{L} I_{gd} - \omega_s I_{gq} \right] \\ V_{gq}^{ref} = -L \left[k_4 e_4 + \frac{dI_{gq}^{ref}}{dt} + \frac{R}{L} I_{gq} + \omega_s I_{gd} - \frac{V_{sq}}{L} \right] \end{cases} \text{with} \begin{cases} e_3 = I_{gd}^{ref} - I_{gd} \\ e_4 = I_{gq}^{ref} - I_{gq} \end{cases} \quad (12)$$

k_5 and k_6 are chosen to be positives parameters.

$$\begin{cases} V_{gd}^{ref} = -L \left[\frac{dI_{gd}^{ref}}{dt} + \frac{R}{L} I_{gd} - \omega_s I_{gq} \right] + L(k_7 e_3 + k_{71} sign(e_3)) \\ V_{gq}^{ref} = -L \left[k_6 e_6 + \frac{dI_{gq}^{ref}}{dt} + \frac{R}{L} I_{gq} + \omega_s I_{gd} - \frac{V_{sq}}{L} \right] + L(k_8 e_4 + k_{81} sign(e_4)) \end{cases} \quad (13)$$

In order to ensure a faster dynamic of the grid current components, k_7, k_{71}, k_8, and k_{81} are chosen to be positives parameters. Therefore:

$$-k_7 e_7^2 - k_{71} e_7 sign(e_7) - k_8 e_8^2 - k_{81} e_8 sign(e_8) < 0 \quad (14)$$

2.2.3. Tracking of the maximum power point of the proposed wind system

In order to extract the maximum power, the specific speed must be set to its optimal value λ_{opt} in order to obtain the maximum power coefficient c_{PMAX}. The power coefficient c_p must be maintained at its maximum value in order to reach the T_{opt}, which is given by (15):

$$T_{opt} = k_{opt} \cdot {\Omega_m}^2 \text{ where, } K_{opt} = \frac{1}{2} \cdot \rho \cdot \pi \cdot R_{blade}^5 \cdot \frac{C_{PMAX}}{{\lambda^3}_{opt}} \quad (15)$$

the tacking error is given by:

$$e = T_{opt} - \hat{T}_m \quad (16)$$

by combining (15), (16) and (4), the dynamics of this error is obtained:

$$\dot{e} = \dot{T}_{opt} - \dot{\hat{T}}_m = 2 \cdot k_{opt} \cdot \Omega_m \cdot (\frac{T_m}{J} - \frac{K}{J} \cdot \Omega_m - \frac{T_{em}}{J}) - \dot{\hat{T}}_m \quad (17)$$

in order to stabilize the system, a Lyapunov function is defined, such as [23]:

$$V = \frac{1}{2}e^2 + \frac{1}{2}\tilde{X}^T P\tilde{X} \quad (18)$$

where P is a positive matrix chosen as follows:

$$H_m^T P + PH_m = -I_2 \quad (19)$$

the dynamics of Lyapunov's function is:

$$\dot{V} = \dot{e} \cdot e - \frac{1}{2}\tilde{X}^T\tilde{X} \quad (20)$$

with a judicious choice of the relationship between the error and its derivative, such as:

$$\dot{e} = -m \cdot e \quad (21)$$

where m is a positive constant.

The (20) becomes:

$$\dot{V} = -m \cdot e^2 - \frac{1}{2}\tilde{X}^T\tilde{X}\langle 0 \quad (22)$$

by combining (17) and (22), the expression of the reference torque can be deduced.

$$T_{em}^{ref} = \hat{T}_m - K \cdot \Omega_m + \frac{J}{2k_{opt}\Omega_m}(m \cdot e - \dot{\hat{T}}_m) \quad (23)$$

Using the same logic as (23), the expression of the backstepping stabilizing command associated with the sliding mode setting is derived as:

$$T_{em}^{ref} = \hat{T}_m - K \cdot \Omega_m + \frac{J}{2k_{opt}\Omega_m}(m \cdot e + n \cdot sign(e) - \dot{\hat{T}}_m) \quad (24)$$

where m and n are positives constants.

2.3. Implementation of the controller's algorithms on DSP

The integration of the DSP card with MATLAB/Simulink software provides a high-performance, high-quality development environment. Co-simulation using the DSP board allows testing a new electronic control unit (ECU) in a virtual environment without real devices or physical machines. After modelling the entire system in Simulink software, the block diagrams of the simulated model can be transferred to DSP via code created by SimulinkCoder. The real-time simulated model is compiled, downloaded, and started automatically. The C2000 library of Texas Instruments DSP family on simulink embedded coder was used to generate the code to be implemented on TMS320L28335 DSP (Figure 2).

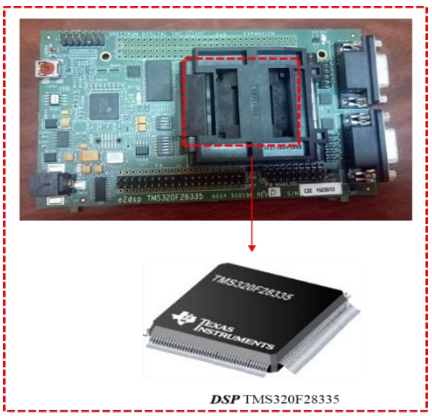

Figure 2. eZDSP TMS320F28335

The main strength of TMS320L28335 DSP lies in the many peripherals it has that has made this DSP a very powerful universal control machine [27]. It has very high performance, so even complex control algorithms can be effectively implemented on this platform. Figure 3 presents the model to be implemented on the DSP and hardware in the loop of the suggested controls. Figure 4 depicts the WECS model under MATLAB/Simulink communicating with the DSP and Figure 5 displays the controls hardware in the loop interacting with MATLAB/Simulink.

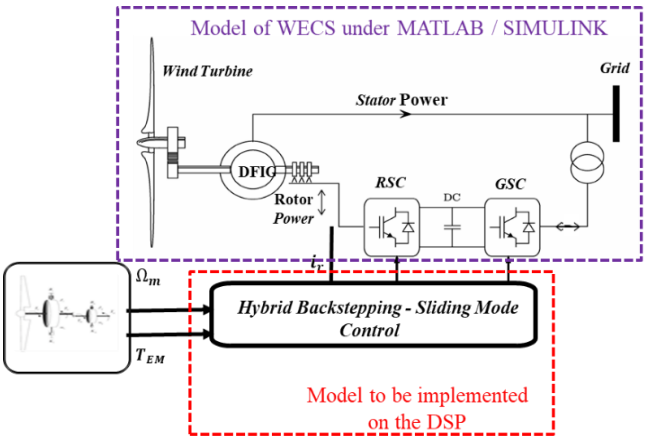

Figure 3. The HIL of the proposed-control algorithms

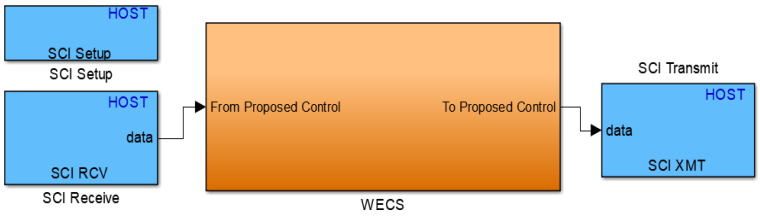

Figure 4. Model of WECS under MATLAB/Simulink

Figure 5. Control algorithms hardware in the loop

3. VALIDATION RESULTS

The proposed algorithm laws are implemented on the TMS320L28335 DSP as a HIL communicating with the WECS model on MATLAB/Simulink. In order to demonstrate the performance and robustness of the proposed strategies, a series of tests have been performed. These tests are performed under the conditions: i) variation of the power setpoint, ii) variation of the speed: at t = 8 [s], →2: 150 [rd/s] → 170 [rd/s], and iii) variation of the DFIG parameter: t = 12 [s], Rr →2* Rr and Lr →2* Lr.

The reference rotor speed and the real measure speed from the proposed controls are shown in Figure 6. The results demonstrate quick convergence and good tracking performance of the real mechanical speed during the whole wind speed profile. The error between the speed reference and the real speed is very small.

The optimal power extracted from the wind turbine by the MPPT algorithm is used as the reference power. Thus, in order to guarantee a unit power factor, it is necessary to have a zero reference for the reactive

power. Figure 7 and Figure 8 show respectively the response of the two powers (active, reactive) of the DFIG, and it can be noted that both powers follow these references successfully, and with a fast response time. Figure 9 and Figure 10 show the waveforms of the currents. The stator and rotor currents both have a sinusoidal waveform. Moreover, the frequency and amplitude of the rotor current vary as a function of the generator speed.

As can be seen in Figure 11, the DC link voltage evolution is extremely satisfactory. The results of the variation of the machine parameters are shown in Figure 12. The DFIG parameter variations show a very small increase in the time response of the proposed control strategy. Furthermore, this result shows a clear effect in steady-state error when using a hybrid control compared to those obtained with a backstepping control strategy [25]. It can be concluded that the proposed control is more robust than the BC. On the other hand, the disadvantage of the sliding mode [14] called chattering phenomenon is overcome by using the hybrid backstepping-sliding mode control. In accordance with the result: i) the results of the implementation of the DSP as a HIL present the performances in terms of set point monitoring, static errors and robustness, and ii) the results of the implementation of the control proposed on DSP as hardware in the loop converge to those obtained with conventional simulations on Simulink.

To validate the performances of the proposed control, a literature review in recent works based on PI regulation of wind energy systems using DFIG [6]-[17] has been done. As a result, for the PI controllers, the effect of the coupling between the two powers is observed because a step imposed on one of the two powers (active or reactive) induces an important dismissal of the powers compared to the reference value and a time to return to the initial state. Thus, during parametric variations, there is an increase in the amplitude of the rejection and in the return time. Therefore, the proposed hybrid strategy shows its superiority by effectively rejecting the effects of disturbances, hence the powers follow their references perfectly. As well as the variations of the parameters of the system have no effect on the evolution of the power.

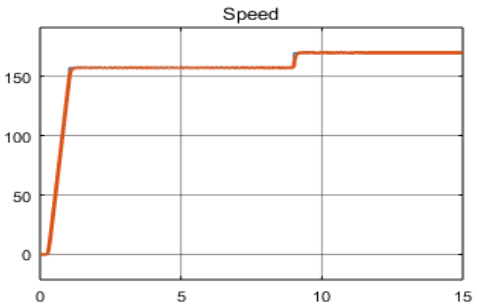

Figure 6. Speed evolution (rad/s)

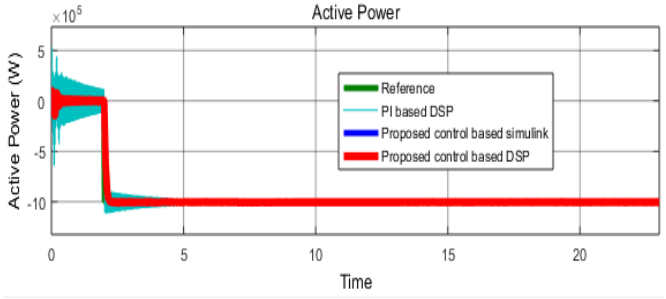

Figure 7. Stator active power evolution

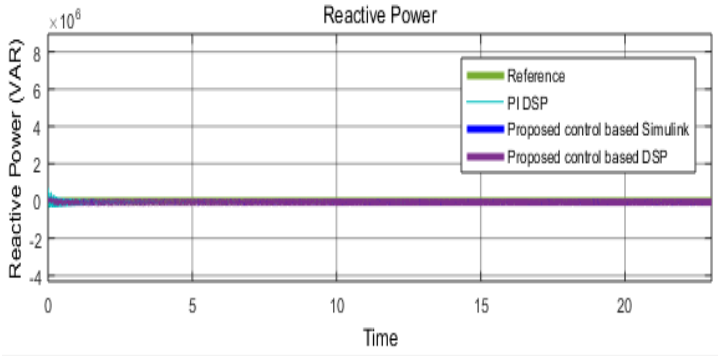

Figure 8. Stator reactive power evolution

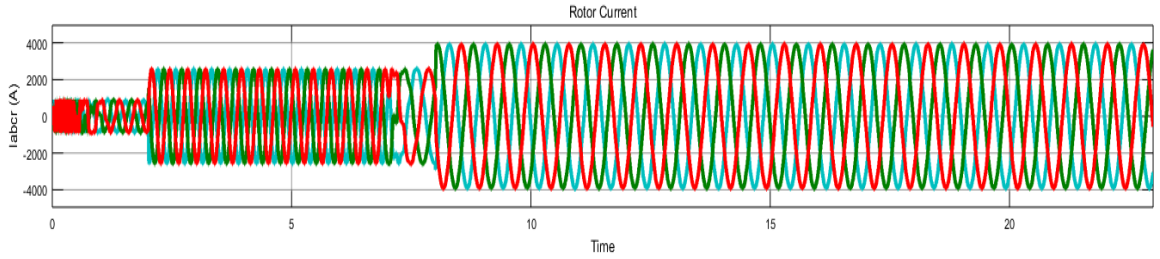

Figure 9. Rotor current evolution

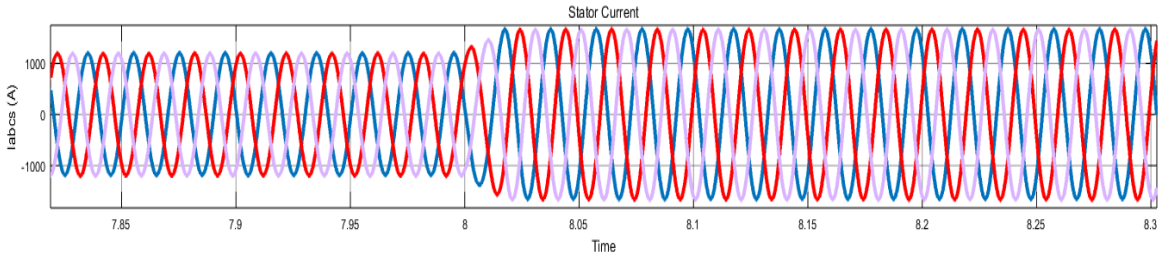

Figure 10. Stator current evolution

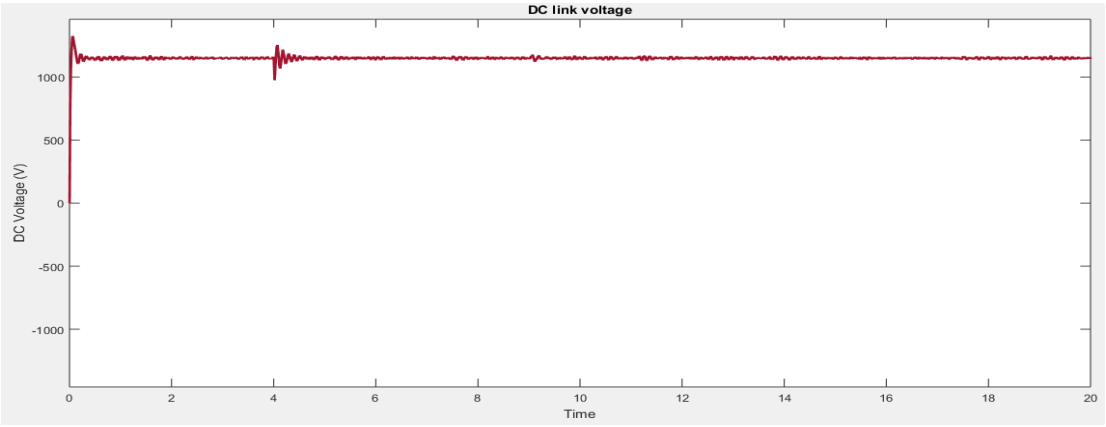

Figure 11. DC-link voltage response

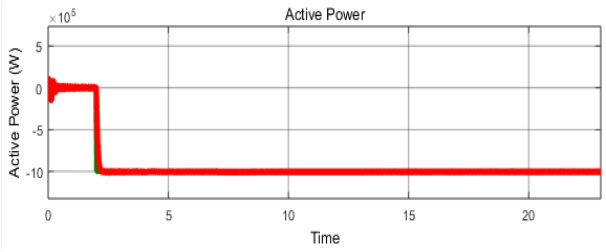

Figure 12. Evolution of the stator power for a 50% variation of the values of Rr and Lr

4. CONCLUSION

This work aimed to improve the performance of a WECS based on a DFIG and to analyse and highlight the contribution of DSP boards in the control of this system. To this end, the work presented in this paper focused on the design and implementation of the WECS control algorithms on the TMS320F28335 DSP board. The main conclusions of this work are: Obtained performances demonstrate that the proposed

nonlinear hybrid approach provides good static and dynamic performances of the system; Setpoint follow-up, robustness and response rapidity are achieved; The results of the implementation of the suggested controls on DSP as HIL confirm the results obtained in Simulink. Accordingly, the effectiveness of this control has been verified.

REFERENCES

[1] G. Abad, *Doubly fed induction machine : Modelling and control for wind energy generation applications*, Wiley-Blackwell Pub, 2011.

[2] A. Tamaarat, and A. Benakcha, "Performance of PI controller for control of active and reactive power in DFIG operating in a grid-connected variable speed wind energy conversion system," *Front. Energy*, vol. 8, no. 3, pp. 371-378, Sep. 2014, doi: 10.1007/s11708-014-0318-6.

[3] H. Q. Minh, N. Frédéric, E. Najib, and H. Abdelaziz, "Power management of a variable speed wind turbine for stand-alone system using fuzzy logic," in *Fuzzy Systems (FUZZ), 2011 IEEE International Conference*, 2011, pp. 1404-1410, doi: 10.1109/FUZZY.2011.6007718.

[4] H. K. Jafari, and A. Radan, "Comparison between self tuning PI voltage control of DFIG and a combinational control for improved wind turbines," *International Journal on Energy Conversion (IRECON)*, vol. 2, no. 5, 2014.

[5] H. Lhachimi, Y. Sayouti, Y. Elkouari, H. Lhachimi, Y. Sayouti, and Y. Elkouari, "The comparison and analysis of the DFIG behavior under PI, fuzzy and sliding mode controllers for wind energy conversion system in the grid connected mode," *Int. Rev. Autom. Control*, vol. 11, no. 3, May 2018, p. 113, doi: 10.15866/ireaco.v11i3.14322.

[6] C. Ahlem, Benretem A, Dobrev I, and B. Barkati, "Comparative study of two control strategies proportional integral and fuzzy logic for the control of a doubly fed induction generator dedicated to a wind application," *International Journal of Power Electronics and Drive Systems (IJPEDS)*, vol. 11, no. 1, pp. 263-274, March 2020, doi: 10.11591/ijpeds.v11.i1.pp263-274.

[7] A. Mseddi, S. Le Ballois, H. Aloui, and L. Vido, "Robust control of a wind conversion system based on a hybrid excitation synchronous generator: A comparison between H∞ and CRONE controllers," *Mathematics and Computers in Simulation*, vol. 6, no. 1, Feb. 2019, pp. 453-476, doi: 10.1016/j.matcom.2018.11.004.

[8] Y.-M. Kim, "Robust data driven H-infinity control for wind turbine," *Journal of the Franklin Institute*, vol. 353, no. 13, pp. 3104-3117, 2016. doi: 10.1016/j.jfranklin.2016.06.009.

[9] M. Benbouzid, *et al*., "AC grid connected DFIG-based wind turbine with shunt active power filter based on nonlinear predictive control," *Int. Rev. Model. Simulations*, vol. 8, no. 3, 2015, doi: 10.15866/iremos.v8i3.6070.

[10] B. Rached, M. Elharoussi, and E. Abdelmounim, "Design and investigations of MPPT strategies for a wind energy conversion system based on doubly fed induction generator," *International Journal of Electrical and Computer Engineering (IJECE)*, vol. 10, no. 5, pp. 4770-4781, 2020, doi: 10.11591/ijece.v10i5.pp4770-4781.

[11] Z. Lahlou, Y. Berrada, and I. Boumhidi, "Nonlinear feedback control for a complete wind energy conversion system," *Int. Rev. Autom. Control*., vol. 12, no. 3, p. 136, May 2019, doi: 10.15866/ireaco.v12i3.16656.

[12] O. Radouane, and M. Rachidi, "Adaptive input-output feedback linearization control of doubly-fed induction machine in wind power generation," *Int. Rev. Autom. Control*., vol. 12, no. 1, p. 11, Jan. 2019, doi: 10.15866/ireaco.v12i1.15619.

[13] N. Khezami, X. Guillaud, and N. Benhadj Braiek, "Multimodel LQ controller design for variable-speed and variable pitch wind turbines at high wind speeds," in *6th International Multi-Conference on Systems, Signals and Devices*, 2009, pp. 1-6, doi: 10.1109/SSD.2009.4956739.

[14] B. Rached, M. Elharoussi, and E. Abdelmounim, "DSP in the loop implementation of sliding mode and super twisting sliding mode controllers combined with an extended kalman observer for wind energy system involving a DFIG," *International Journal on Energy Conversion (IRECON)*, vol. 8, no. 1, pp. 26-37, 2020, doi: 10.15866/irecon.v8i1.18432.

[15] M. Reddak, A. Berdai, A. Gourma, J. Boukherouaa, and A. Belfiqih, "Enhanced sliding mode MPPT and power control for wind turbine systems driven DFIG (doubly-fed induction generator)," *Int. Rev. Autom. Control*., vol. 9, no. 4, p. 207, Jul. 2016, doi: 10.15866/ireaco.v9i4.9739.

[16] A. Kalantar Zadeh, L. I. Kashkooli, and S. A. Mirzaee, "Designing a power inverter and comparing back-stepping, slinding-mode and fuzzy controllers for a single-phase inverter in an emergency power supply," *Ciencia e Natura*, vol. 37, no. 2, pp. 175-181, 2015, doi: 10.5902/2179460X20769.

[17] B. Rached, M. Elharoussi, and E. Abdelmounim, "Fuzzy logic control for wind energy conversion system based on DFIG," in *2019 International Conference on Wireless Technologies, Embedded and Intelligent Systems (WITS)*, 2019, pp. 1-6, doi: 10.1109/WITS.2019.8723722.

[18] Edgar N. Sanchez, and Riemann Ruiz-Cruz, *Doubly fed induction generators: control for wind energy*, Boca Raton, Florida, USA: CRC Press Taylor and Francis Group, 2016.

[19] O. P. Bharti, R. K. Saket, and S. K. Nagar, "Controller design for DFIG driven by variable speed wind turbine using static output feedback technique," *Engineering, Technology & Applied Science Research*, vol. 6, no. 4, pp. 1056-1061, 2016, doi: 10.5281/zenodo.60980.

[20] N. R. Babu, and P. Arulmozhivarman, "Wind energy conversion systems-technical review," *Journal of Engineering Science and Technology*, vol. 8, no. 4, pp. 493-507, 2013.

[21] G. S. Kaloi, J. Wang, and M. H. Baloch, "Active and reactive power control of the doubly fed induction generator based on wind energy conversion system," *Energy Reports*, vol. 2, Nov. 2016, pp. 194-200, doi: 10.1016/j.egyr.2016.08.001.

[22] S. K. El Khil, I. Slama-Belkhodja, M. Pietrzak-David, and B. de Fornel, "Power distribution law in a doubly fed induction machine," *Math. Comput. Simul*., vol. 71, no. 4-6, pp. 360-368, Jun. 2006, doi: 10.1016/j.matcom.2006.02.019.
[23] B. Beltran, M. E. H. Benbouzid, and T. Ahmed-Ali, "A combined high gain observer and high-order sliding mode controller for a DFIG-based wind turbine", in *2010 IEEE International Energy Conference*, Manama (Bahraïn), December 2010, pp. 322-327, doi: 10.1109/ENERGYCON.2010.5771699.
[24] B. Beltran, M. E. H. Benbouzid, and T. Ahmed-Ali, "Second-order sliding mode control of a doubly fed induction generator driven wind turbine," I*EEE Trans. Energy Convers*., vol. 27, no. 2, pp. 261-269, Jun. 2012, doi: 10.1109/TEC.2011.2181515.
[25] B. Rached, M. Elharoussi, and E. Abdelmounim, "DSP in the loop implementation of a backstepping controller for wind energy conversion system based on a doubly fed induction generator connected to grid," *International Journal on Energy Conversion (IRECON)*, vol. 7, no. 4, p. 136, 2019, doi: 10.15866/irecon.v7i4.17790.
[26] S. Boubzizi, H. Abid, A. El hajjaji, and M. Chaabane, "Comparative study of three types of controllers for DFIG in wind energy conversion system," *Protection and Control of Modern Power Systems*, vol. 3, no. 1, 2018, doi: 10.1186/s41601-018-0096-y.
[27] A. Elrajoubi, S. S. Ang and A. Abushaiba, "TMS320F28335 DSP programming using MATLAB Simulink embedded coder: Techniques and advancements," in *2017 IEEE 18th Workshop on Control and Modeling for Power Electronics (COMPEL)*, 2017, pp. 1-7, doi: 10.1109/COMPEL.2017.8013418.

BIOGRAPHIES OF AUTHORS

Bouchaib Rached was born in El jadida, Morocco. He is a PhD student in the Laboratory of Signal Analysis and Information Processing, FST Settat, Hassan 1st University, Morocco. He received an engineer's degree in Electrical Engineering from Mohammadia School of Engineering Morocco in 2012. His research activities include the design and the application of robust digital control in the wind turbine power systems based on Doubly Fed Induction Generator connected to the grid. He also has research interest ranging from signal processing to industrial application of Automatic Control.

Mustapha Elharoussi was born in Azilal Morocco in 1974; he received his PhD in Error Correcting Codes from Mohammed V University Morocco in 2013. In 2014 he joined, as Professor, applied Physics department of FST, Hassan I University, Settat, Morocco.

Elhassane Abdelmounim, received his PhD in applied Spectral analysis from Limoges University at science and technical Faculty, France in 1994. In 1996, he joined, as Professor, applied physics department of science and technical faculty, Hassan 1st University, Settat, Morocco. His current research interests include digital signal processing and machine learning. He is currently coordinator of a Bachelor of Science in electrical engineering and researcher in "ASTI" System Analysis and Information Technology Laboratory at science and technical faculty, Hassan 1st University, Settat, Morocco.